CFD simulations of extreme thunderstorm downburst winds

Josip Žužul[1]*, Alessio Ricci[2,3], Massimiliano Burlando[1]

[1] *Department of Civil, Chemical and Environmental Engineering, University of Genoa, Genoa, Italy*
[2] *Department of Civil Engineering, KU Leuven, Leuven, Belgium*
[3] *Department of the Built Environment, Eindhoven University of Technology, Eindhoven, the Netherlands*
*__Corresponding author__: josip.zuzul@edu.unige.it

Abstract
Thunderstorms are non-synoptic wind events with potentially devastating implications for the integrity of low and mid-rise structures. Thunderstorm outflows commonly referred to as downbursts are characterized by a vertical cold air impingement from the cloud to the surface of the Earth accompanied with a divergent radial outflow dominated by the primary ring vortex. This study aims to investigate the physical characteristics of downbursts in the perspective of wind-induced structural loading. Two downburst scenarios were considered: (*Case 1*) an isolated downburst wind, and (*Case 2*) a downburst immersed in an approaching atmospheric boundary layer (ABL) wind. For that purpose, the experimental tests that were previously performed in WindEEE Dome were recreated through Computational Fluid Dynamics (CFD) simulations. Both *Case 1* and *Case 2* were successfully validated with experiments in terms of vertical profiles of radial velocity. All three utilized CFD approaches (URANS, SAS and LES) showed decent performance. However, the LES demonstrated its superiority over the former two in terms of obtaining physically most meaningful representation of complex downburst flow conditions.

Keywords
Thunderstorm downbursts, CFD simulations, WindEEE Dome, ABL-downburst wind interaction

1. Introduction

Severe non-synoptic winds with thunderstorm-related origin (downbursts and tornados) are known for their potential to create significant damage to low-rise structures [1]. In that regard, the most recent ASCE 7-22 standards have been updated to account for tornados, while the Eurocode is about to follow the same example [7]. A similar approach for downbursts is however still not present [9], implying that further research on downbursts is necessary. In the most simplified case, the physical characteristics of a downburst are defined through the vertical cold air impingement from the storm that produces the primary ring vortex which leads to the strong diverging winds close to the surface [3]. However, a realistic downburst would rather incorporate the additional contribution of the atmospheric boundary layer (ABL) winds in which it is commonly immersed. This contribution of ABL winds causes the downburst flow field to deflect from the theoretically symmetric one found in the isolated storms. This therefore yields a requirement for a comparative study of flow field behavior between these two scenarios in the perspective of identifying the worst conditions in terms of wind loading of structures. In this work two downburst scenarios were selected for the investigation of flow characteristics: (*i*) an isolated downburst wind, and (*ii*) a downburst immersed in an approaching ABL wind. This study was conducted within the framework of the Project "THUNDERR – Detection, simulation, modelling and loading of thunderstorm outflows to design wind-safer and cost-efficient structures" [8, 10] and its focus was on the reconstruction of the experimental tests by means of Computational Fluid Dynamics (CFD) technique. In that perspective, the experimental tests previously performed in the WindEEE Dome - a specialized facility for reconstructing downbursts at reduced scales [2], were used as the baseline for CFD analyses. Several CFD approaches were utilized in this study: (*i*) unsteady Reynolds-Averaged Navier-Stokes (URANS), (*ii*) Scale-Adaptive Simulations (SAS), and (*iii*) Large-Eddy Simulations (LES). The selected CFD approaches were also used for the

formulation of best-practice guidelines in the application of the CFD technique for downburst winds. The paper is organized as follows: Section 2 provides the overview of baseline experimental downburst scenarios (isolated downburst, and downburst immersed in an approaching ABL) that were used in the numerical studies. Section 3 summarizes the numerical settings used to conduct the CFD analyses. Section 4 presents the comparison of CFD results with experiments. Finally, Section 5 summarizes the results and presents future work perspectives.

2. Experimental tests

The experimental tests of both isolated thunderstorm downburst and a downburst immersed in an ABL wind were carried out at the WindEEE Dome [2]. The WindEEE Dome is a closed-circuit facility of a hexagonal shape that recreates the near-surface downburst flow through the jet impingement from the nozzle. Conversely, for the generation on ABL-like winds it utilizes 60 fans placed at one sidewall of the chamber (Figure 1). For the isolated downburst tests (*Case 1*), the vertical inflow jet velocity w_{jet} of 9 m/s was released through the inflow jet nozzle of 3.2 m diameter (D). Following the jet release, the primary vortex (PV) forms and the near-surface flow features representative of the full-scale downbursts are recreated. The jet release duration in the chamber was 4 seconds, while the total duration of the experiment was 10 seconds. The experimental campaign made use of a set of Cobra probes placed on a measurement rake to record the radial velocity during the event. The measurement rake was placed at various radial R/D locations (distanced from the chamber center). Experiments were repeated 20 times to obtain a greater degree of statistical significance. In order to recreate the interaction between two wind types (*Case 2*), the experimental tests were performed in two phases. Firstly, the ABL-like wind was developed in the chamber for 24 seconds (two flow-through times), by means of frictional effects induced by the (almost) completely smooth chamber surface. Next, the downburst was released through the vertical jet impingement from the nozzle (w_{jet} of 12 m/s) in the same way as for (*Case 1*). The experimental campaign utilized two sets of Cobra probes to record the velocity time histories: (*i*) Cobras pointing in the direction of the ABL-like wind, and (*ii*) Cobras pointing towards the chamber center to record the downburst-related radial velocities. Cobra probes were mounted on a measurement rake placed across various azimuthal locations α (with respect to the approaching ABL) and radial R/D locations (distanced from the chamber center). The experiments were repeated 10 times to obtain a better statistical representation of the phenomenon. (*Case 1*) considered only the azimuthal position α of 0° due to the assumed flow axisymmetry.

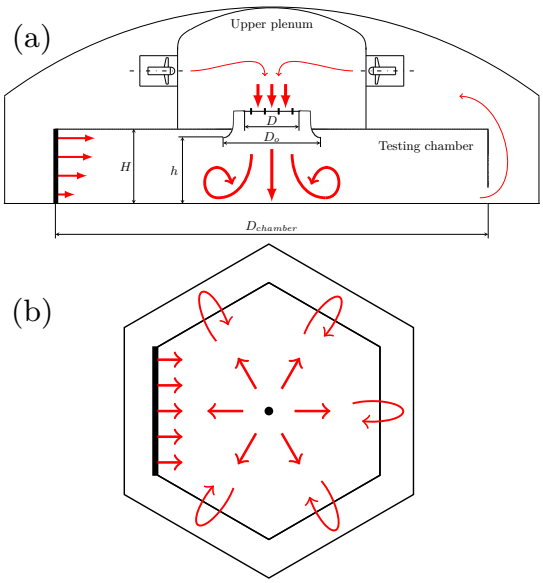

Figure 1. WindEEE Dome facility schematic: (a) front view and, (b) top view of the testing chamber.

3. CFD simulations

3.1 Isolated downburst wind

CFD simulations for the isolated downburst were performed at a computational grid (16.5 million hexahedral cells) representing half of the WindEEE Dome chamber, by taking advantage of the symmetry constraint in order to save computational resources. Wall boundaries were treated with the no-slip condition, while zero-static gauge pressure was specified at the outlet. The near-wall flow was modeled using the Spalding wall functions for smooth surfaces. The PISO-algorithm based solver was adopted to couple pressure and velocity fields, with the usage of second-order discretization schemes. Three CFD approaches were used: URANS, SAS, and LES. The URANS (and SAS) utilized the $k-\omega$ SST turbulence model, while the LES employed the dynamic sub-grid scale turbulence model for the evaluation of Smagorinsky constant through Lagrangian averaging process [5]. The inflow turbulence for LES simulation case was synthesized by adopting the anisotropic turbulent spot method by Kröger and Kornev [4]. Simulations were performed in two stages: (*i*) with the fixed mean vertical inflow velocity of 9 m/s at the nozzle, and (*ii*) with the zero-inflow velocity (*i.e.* by keeping the inflow through the nozzle closed) that would account for the

gradual event dissipation.

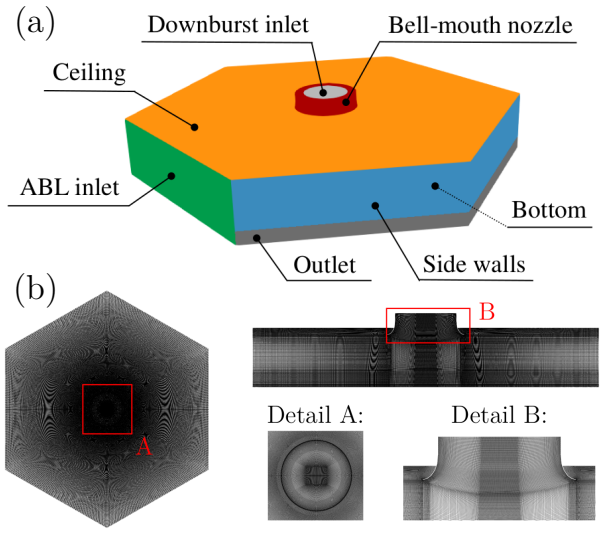

Figure 2. Computational domain with the intication of boundaries for the *Case 2* (a), and corresponding computational grid (b).

3.2 Downburst immersed in an ABL wind

To accurately perform complex downburst-ABL wind interaction, the appropriate approach ABL profile was characterized at the inlet of the computational domain representing the WindEEE Dome testing chamber. The constructed structured grid was composed of 33 million elements described the entire WindEEE Dome testing chamber (Figure 2). The analogous domain and grid configuration (just half of it) was used for the *Case 1*. CFD simulations (URANS, SAS, and LES) were performed in accordance with the experimental campaign: (*i*) ABL-like flow was developed and initialized in the domain, and (*ii*) downburst jet was released from the nozzle inlet with the average vertical jet velocity (w_{jet}) of 12 m/s on the top of the background ABL-like wind. Similarly to the isolated downburst *Case 1*, the $k-\omega$ SST turbulence model was used for the URANS and SAS, while the dynamic model with Lagrangian averaging was used to account for the subgrid scale turbulence in LES simulations. Spatially and temporally correlated turbulent structures needed for the LES simulations at both ABL and downburst inflow faces was introduced through the turbulent inflow generator proposed by Poletto et al. [6]. Wall functions for the atmospheric flows were used at the bottom surface, while the Spalding wall functions were utilized at other wall-type boundaries. Other settings are similar to the ones already introduced for the isolated downburst case: zero-static gauge pressure at the outlet, the second-order discretization schemes were used for the equations and the PISO algorithm-based solver was used to couple pressure and velocity fields.

4. Results

4.1 Isolated downburst wind

CFD results and measured data are compared in terms of vertical profiles of radial velocity component (u) at the selected radial position, *i.e.* in the vicinity of the maximum radial velocity occurrence ($R/D = 1.2$). The comparison is presented in Figure 3 for the selected non-dimensional time steps τ, defined as $\tau = w_{\text{jet}} \cdot t/D$. The velocity u was hereby normalized with the maximum radial velocity registered in LES simulations U_{max}, while the height z was normalized with the height Z_{max} corresponding to the Umax. The measured data is indicated with black dots (ensemble mean across all repetitions) with two-sided error bars of the experimental variability (*i.e.* maximum and minimum occurrence across all repetitions). The CFD simulations generally show acceptable degree of accuracy by falling within the error bars of experimental repetitions throughout the majority of selected time steps. However, URANS and SAS tend to overestimate ($\tau = 4.725$, $\tau = 6.975$) and underestimate ($\tau = 5.2875$, $\tau = 5.85$) the velocity profile during the primary vortex passage, when compared to both experiments and LES. Although all three used CFD approaches provided decent accuracy, the LES simulations show superior behavior by consistently representing the physical behavior of the experimental downburst.

4.2 Downburst immersed in an ABL wind

Figure 4 shows the comparison of measured data with simulated vertical profiles (URANS, SAS, and LES cases) of radial velocity (u) at the rear side ($\alpha = 180°$) at $R/D = 1.4$, and for the selected set of non-dimensional time steps τ. This particular location was selected since the U_{max} was registered in its vicinity (in LES simulations). Additionally, the vertical profiles associated with the isolated jet were also presented to allow for the comparison in terms of profile change due to the presence of the ABL-like winds. In general, the measured and simulated profiles show a very good agreement across all positions of Cobra probes, and across all selected time instances τ. The vertical profiles at $\alpha = 180°$ are found to have a less pronounced nose due to higher values observed at upper levels with respect to profiles at $\alpha = 0°$ (not presented here), which are caused by the higher level ABL winds. Although URANS and SAS approaches gave promising results for the general flow understanding, they are found to have a tendency for the overestimation of the velocity peak associated with the PV passage (not presented

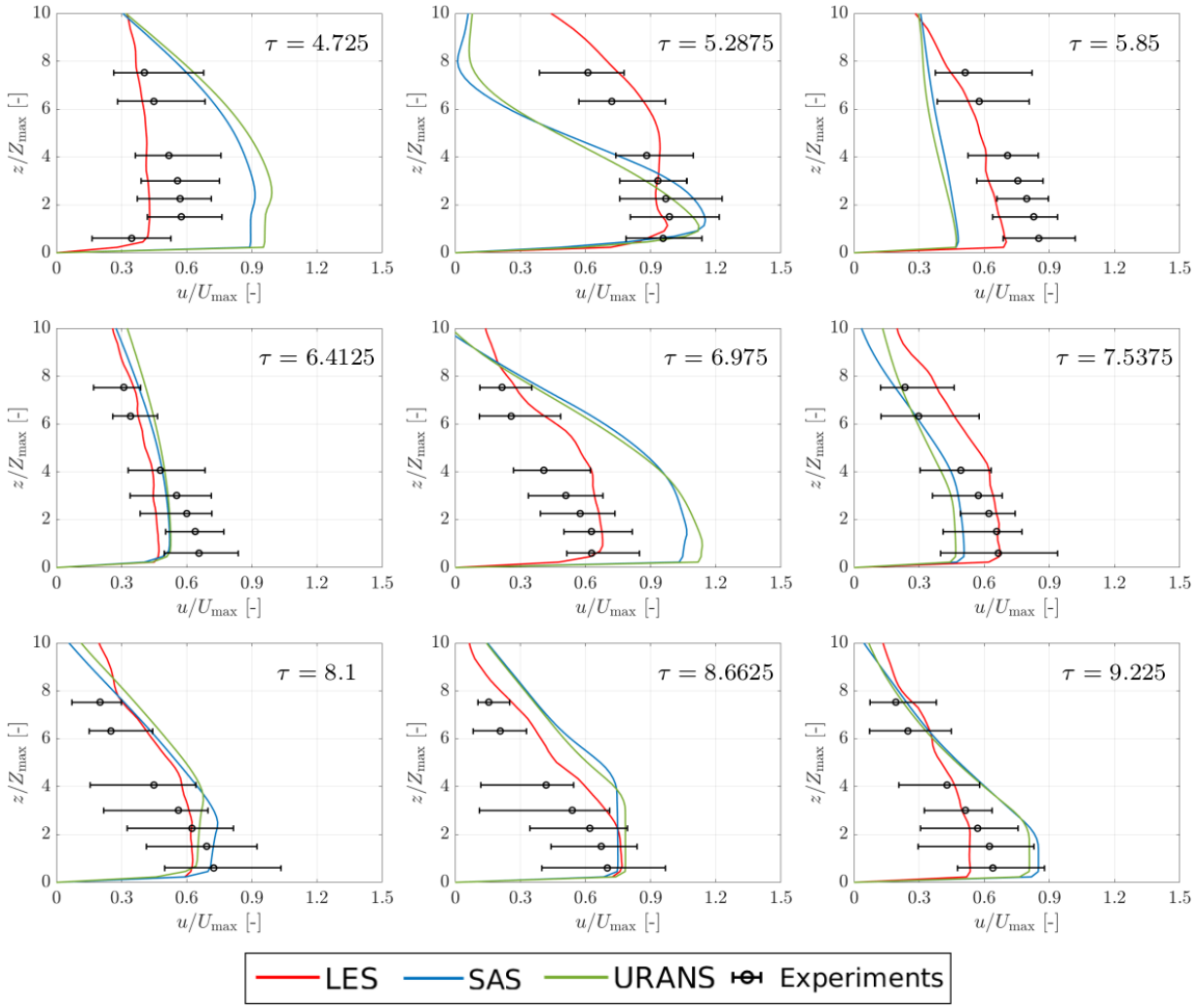

Figure 3. Comparison of measured data with simulated vertical profiles of radial velocity at radial location R/D = 1.2 for a set of non-dimensional time steps (τ).

here). Conversely, LES simulations showed consistent superior performance when compared to the URANS and SAS, and are therefore considered a favorable CFD approach for numerical description of downburst flows in conjuction with the ABL-like winds.

5. Conclusions and future work perspectives

The study presented in this work was conducted under the umbrella of the Project "THUNDERR – Detection, simulation, modelling and loading of thunderstorm outflows to design wind-safer and cost-efficient structures" [8, 10] and it focused on the numerical reconstruction of reduced scale experimental tests previously performed in the WindEEE Dome. In particular, two reduced-scale experimental downburst scenarios were recreated through the application of the CFD technique: (*i*) an isolated downburst wind (*Case 1*), and (*ii*) a downburst immersed in an approach ABL wind (*Case 2*). Both campaigns were recreated through URANS, SAS, and LES approaches, and the numerical results were compared with the measurements in the form of vertical profiles of radial velocity at radial locations (R/D) in the proximity of the location where strongest winds were observed. The comparison with the measurements demonstrated that all three utilized CFD approaches can provide a reasonable degree of accuracy for both analyzed scenarios in terms of a trend of vertical profiles in time. However, the URANS and SAS were found to lack consistency in adequately describing the primary vortex passage. That defficiency in turn resulted in the overestimation and underestimation of the associated radial velocity. Conversely, LES showed a consistent trend and accuracy in predicting the strongest winds in complex flow conditions. Compared to the *Case 1* which showed the axisymmetric flow behavior, the scenario of a downburst immersed in an ABL wind has an emphasized flow asymmetry. All three employed CFD approaches on average provided similar acceptable behavior as in the case of an iso-

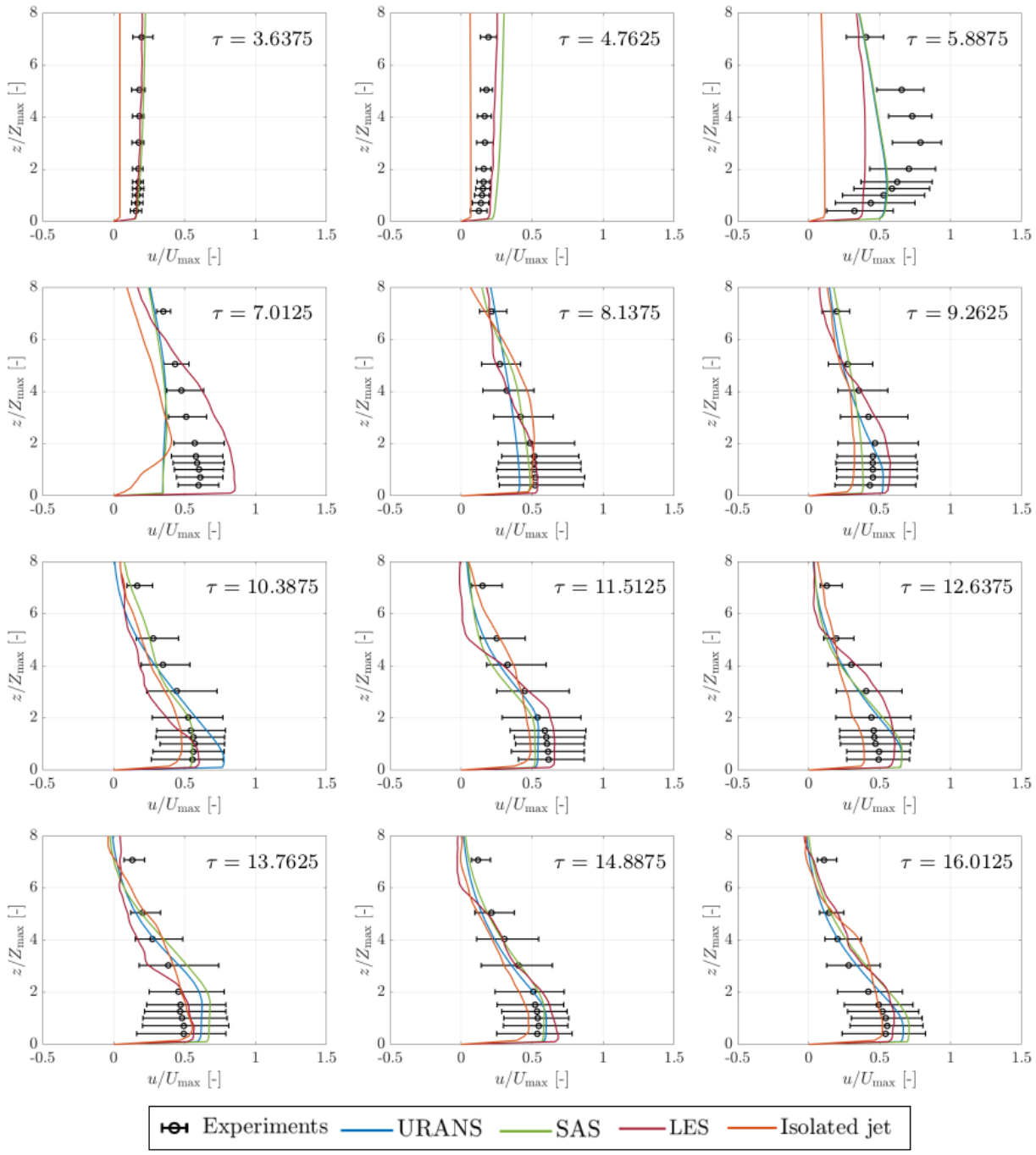

Figure 4. Comparison of measured and simulated vertical profiles of radial velocity at $\alpha = 180°$ and $R/D = 1.4$ for a selected set of non-dimensional time steps (τ).

lated downburst, while the LES once again showcased its superior behavior when compared to the URANS and SAS. In particular, LES showed a consistent and high degree of accuracy in predicting wind velocities regardless of the azimuthal location. In the perspective of importance of downburst winds for structural safety in thunderstorm-prone regions, the future work will be directed towards the CFD reconstruction of full-scale downburst events instead of focusing on reduced-scale experimental campaigns. Therefore, the selected full-scale downburst event recorded in a complex urban environment will be reconstructed in order to firstly validate the applicability of the commonly used impinging jet model, and finally to obtain its full-field flow features and its characteristics at larger scales.

References

[1] T. T. Fujita. “Tornadoes and Downbursts in the Context of Generalized Planetary Scales”. In: *Journal of the Atmospheric Sciences* 38.8 (1981), pp. 1511–1534.

[2] H. Hangan et al. “Novel techniques in wind engineering”. In: *Journal of Wind Engineering and Industrial Aerodynamics* 171 (2017), pp. 12–33.

[3] M. Hjelmfelt. “Structure and Life Cycle of Microburst Outflows Observed in Colorado”. In: *Journal of Applied Meteorology* 27 (1988), pp. 900–927.

[4] H. Kröger and N. Kornev. “Generation of divergence free synthetic inflow turbulence with arbitrary anisotropy”. In: *Computers and Fluids* 165 (2018), pp. 78–88.

[5] C. Meneveau, T. Lund, and W. Cabot. “A Lagrangian dynamic subgrid-scale model of turbulence”. In: *Journal of Fluid Mechanics* 319 (1996), pp. 353–385.

[6] R. Poletto, T. Craft, and A. Revell. “A new divergence free synthetic eddy method for the reproduction of inlet flow conditions for LES flow”. In: *Turbulence and combustion* 91.3 (2013), pp. 519–539.

[7] F. Ricciardelli. “Towards the Second Generation Eurocodes: the role of research in the updating of wind loading codes”. In: *Keynote lecture of the In-Vento 2022: 16th Conference of the Italian Association for Wind Engineering* (4 – 7 September 2022, Milano, Italy).

[8] G. Solari, M. Burlando, and M. P. Repetto. “Detection, simulation, modelling and loading of thunderstorm outflows to design wind-safer and cost-efficient structures”. In: *Journal of Wind Engineering and Industrial Aerodynamics* 200 (2020), pp. 104–142.

[9] T. Stathopoulos and H. Alrawashdeh. “Wind loads on buildings: A code of practice perspective”. In: *Journal of Wind Engineering and Industrial Aerodynamics* 206 (2020), p. 104338.

[10] THUNDERR. URL: http://www.thunderr.eu. Accessed: October 10, 2022.